

Cite this: *Polym. Chem.*, 2021, **12**, 4253Received 4th June 2021,
Accepted 6th July 2021

DOI: 10.1039/d1py00753j

rsc.li/polymers

Polymers from sugars and CS₂: ring opening co-polymerisation of a D-xylose anhydrosugar oxetane†Thomas M. McGuire  and Antoine Buchard  *

A D-xylose anhydro sugar derivative (**1**) has been applied in the ring-opening copolymerisation (ROCOP) with CS₂ to form a polythiocarbonate (poly(CS₂-co-**1**)) with high head-head/tail-tail regioselectivity towards alternating thiono- and trithiocarbonate linkages (up to 95%). Through variation of the reaction parameters (e.g. temperature and CS₂ stoichiometry), some control over the regioselectivity (head-head/tail-tail linkages 57–95%) and the nature of the polymer linkages is possible. Conditions can also be tailored to enable the facile isolation of a polymerisable cyclic xanthate, **2**. Kinetic experiments suggest that across the range of temperatures studied, the formation of poly(CS₂-co-**1**) proceeds at least partially by direct copolymerisation of **1** and CS₂, without necessarily going through the ring-opening polymerisation (ROP) of **2**. Poly(CS₂-co-**1**) exhibits partial chemical recyclability into cyclic monomer **2** (up to 45% after 20 h at 110 °C with [poly(CS₂-co-**1**)]₀ = 1.34 mol L⁻¹). Finally, rapid degradation (<1 h) of poly(CS₂-co-**1**) is possible under UV radiation (λ = 365 nm) and is accelerated in the presence of tris(trimethylsilyl)silane (TTMSS).

Introduction

Owing to the environmental issues surrounding plastic use, a societal shift away from traditional petroleum-derived feedstocks is driving innovation in the field of sustainable polymer chemistry. Polymers derived from sugars have huge potential as sustainable alternatives to current commodity plastics.^{1–5} For instance, polymers which incorporate pyranose or furanose motifs typically exhibit remarkably high glass transition temperatures (*T*_g) and the availability of hydroxyl groups of sugar derivatives significantly broadens the scope for prospective material functionalisation.^{6–9}

It is known that the replacement of oxygen atoms with sulfur ones in oxygenated polymers can give the resulting polythioethers, polythiocarbonates and polythioesters enhanced physical and thermal properties,^{10–16} as well as additional advanced optical¹⁷ and electrical characteristics.¹⁸ Moreover, sulfur-containing polymers exhibit biocompatibility and have shown potential in metal and bacterial adhesion.^{19,20} The presence of sulfur atoms in the backbone of polymers may also accelerate degradation under appropriate conditions (e.g. under UV radiation).^{19,21}

The synthesis of polythiocarbonates is possible through polycondensation,^{22–25} the ring-opening polymerisation (ROP) of cyclic thiocarbonates,^{26,27} polyalkylation of trithiocarbonates^{28,29} or the ring-opening copolymerisation (ROCOP) of CS₂^{15,30–33} and COS^{11,34–38} with cyclic ethers (epoxides and oxetane). ROCOP methods are particularly interesting given the array of synthetic possibilities provided by the pool of cyclic ethers usable, coupled with the polymerisation control brought by existing ROCOP catalysts.^{39,40} To date, both heterogeneous (e.g. Zn–Co(III) double-metal cyanide complexes)⁴¹ and homogeneous catalysts/initiators (e.g. metal salen/onium catalysts^{30,34,42} and LiO^tBu³¹) have been reported for CS₂/cyclic ether ROCOP. However, reports of ROCOP between an oxetane and CS₂ remain rare.³²

CS₂ is manufactured by reaction of charcoal or natural gas with sulfur, and despite its known toxicity, incorporating it into polymers has some benefits in terms of waste valorisation. Indeed, sulfur is an abundant by-product of the oil and chemical industry.^{43–45} Our group has previously used CS₂ to synthesise a series of cyclic thiocarbonates for ROP towards sugar-derived polythiocarbonates.²⁷ However, the synthesis of these monomers was challenging, necessitating extensive purification (e.g. successive column chromatography) to be suitable for ROP techniques. For xylose-derived xanthate monomer, **2**, ROP towards poly(**2**) formed a regioregular polymer with up to 87% head-head/tail-tail (HH/TT), trithiocarbonate/thionocarbonate linkages, although no control over the polymer microstructure was demonstrated.

It was envisioned that the ROCOP of CS₂ with oxetane-functionalised xylofuranose derivative, **1**, may expediate the polymer synthesis given its ease of preparation in purities suit-

Centre for Sustainable and Circular Technologies, Department of Chemistry,
University of Bath, Claverton Down, Bath BA2 7AY, UK.

E-mail: a.buchard@bath.ac.uk

†Electronic supplementary information (ESI) available: Experimental procedures, NMR spectra of polymers and degradation products. SEC, TGA-MS, WAXS and DSC traces. *M*_n plots and mechanistic considerations. See DOI: 10.1039/d1py00753j

able for ROP⁴⁶ and ROCOP.⁴⁷ Moreover, we hypothesised that alternative polymer sequences may be accessible through ROCOP. Lastly, through judicious choice of conditions, it was hoped that the reaction between CS₂ and **1** could be tailored towards cycloaddition over copolymerisation, to access **2** with fewer purification steps.

We have previously used 1,2-cyclohexanediamino-*N,N'*-bis(3,5-di-*t*-butylsalicylidene)-chromium(III), **CrSalen** and bis(tri-phenylphosphine)iminium chloride (PPNCl) to catalyse the ROCOP of cyclic anhydrides and **1** for the preparation of polyesters.⁴⁷ **CrSalen**/onium salts (PPNN₃) binary catalytic system has also been applied in the ROCOP of oxetane with CS₂. Detailed study revealed the presence of multiple polymer linkages indicative of sulfur/oxygen scrambling which became more prevalent at higher temperatures.³² Werner and co-workers have reported on the ROCOP of terminal epoxides with CS₂ initiated by Li⁺OBu.³¹ The polythiocarbonates were found to be highly regioregular with up to 94% head-head/tail-tail alternating thionocarbonate/trithiocarbonate linkages.

Herein we describe the ROCOP of **1** with CS₂ to form sugar-based sulfur-containing polymers with very high regioselectivity towards HH/TT, trithiocarbonate/thionocarbonate linkages (up to 95%), marking an improvement on the similar polymer synthesised through the ROP of **2**. The head/tail configuration of poly(CS₂-co-**1**) can be varied through modulation of the reaction temperature and CS₂ stoichiometry. Mechanistic investigations show that ROCOP proceeds at least partially directly. Lastly, poly(CS₂-co-**1**) exhibits partial chemical recyclability into **2**, as well as full degradation under UV light.

Results and discussion

Poly(CS₂-co-**1**) made by ROCOP: identification of polymer linkages

Oxetane **1** was synthesised in three steps from D-xylose in accordance with previous reports (51% overall yield).^{46,47} ROCOP was initially trialed with **CrSalen** and PPNCl with [1]₀: [CS₂]₀: [CrSalen]₀: [PPNCl]₀ loadings of 100:200:1:1 at 80 °C. In contrast with other polymerisations developed with **1** so far,^{46–49} the reaction proceeded readily at relatively mild temperatures, with 33% conversion of **1** after 4.5 h at 80 °C to yield poly(CS₂-co-**1**) of 2800 g mol^{−1} (*D*_M = 1.54; measured by size-exclusion chromatography (SEC)). The formation of resonances at 192.9 ppm (**S1**) and 222.4 ppm (**S2**) in the ¹³C{¹H} NMR spectrum and 5.52 ppm and 5.80–6.03 ppm in the ¹H NMR spectrum suggested the incorporation of CS₂ within the polymer backbone, later confirmed by ¹H-¹³C{¹H} HSQC and HMBC experiments (Scheme 1, Fig. 1 and 2). ¹H and ¹H-¹³C{¹H} HMBC NMR spectra indicated that the ROCOP of CS₂ and **1** was ring-selective, with CS₂ incorporation across the oxetane moiety only. Furthermore, the ¹H-¹³C{¹H} HMBC NMR spectrum of isolated and crude poly(CS₂-co-**1**) revealed correlations between carbon resonance **S1** and proton environment **c** (*i.e.* the CH in position 3 on the xylofuranose core), and between



Scheme 1 Possible products and linkages formed during the ROCOP of **1** and CS₂.



Fig. 1 ¹H NMR spectra (400 MHz, CDCl₃) of (a) isolated poly(CS₂-co-**1**), (b) **2**, (c) **1** and (d) crude poly(CS₂-co-**1**) (33% conv of **1**); (e) ¹³C{¹H} NMR spectrum (126 MHz, CDCl₃) of isolated poly(CS₂-co-**1**). Reaction performed neat at 80 °C with [1]₀: [CS₂]₀: [CrSalen]₀: [PPNCl]₀ loadings of 100:200:1:1 for 4.5 h.

carbon resonance **S2** and proton environment **e** (*i.e.* the CH₂ in position 6 on the xylofuranose core), consistent with HH/TT configuration and alternating thiono- and trithiocarbonate linkages. Overall, the NMR spectroscopic data for poly(CS₂-co-**1**) was similar to that of the regioregular polymer obtained previously by ROP of **2** (Table 2, entry 1).²⁷

Minor resonances associated with the **e** environment were also observed between δ = 2.65–3.13 ppm and δ =



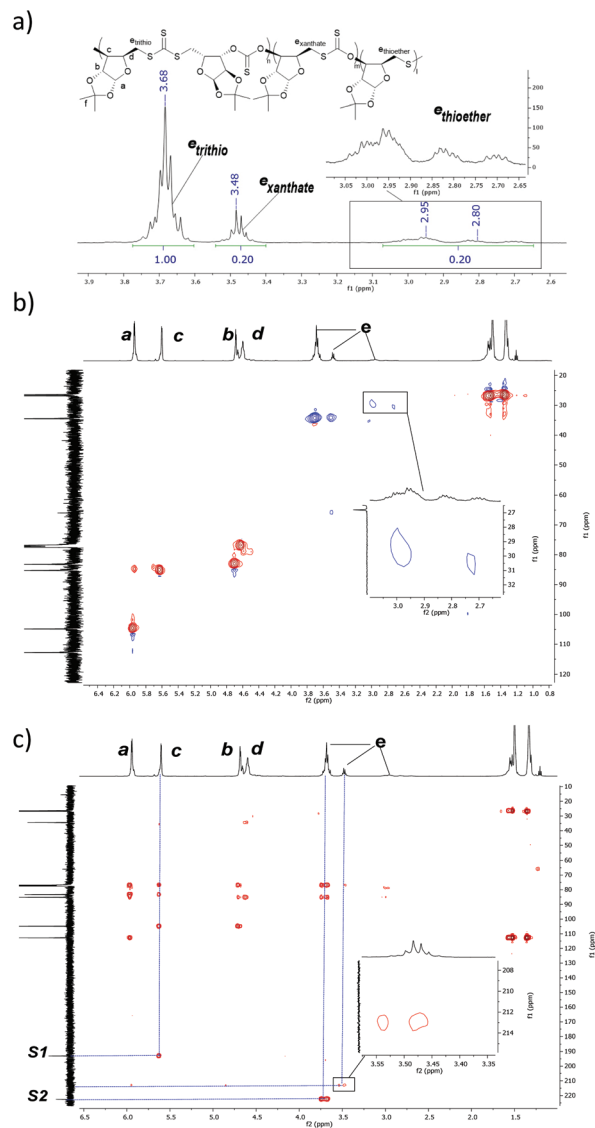


Fig. 2 (a) ^1H NMR (500 MHz, CDCl_3) and (b) ^1H - ^{13}C HSQC (500 MHz, CDCl_3) spectra of isolated poly(CS_2 -co-1) formed neat at 80 °C with $[\mathbf{1}]_0 : [\text{CS}_2]_0 : [\text{CrSalen}]_0 : [\text{PPNCl}]_0$ loadings of 100 : 200 : 1 : 1. (c) ^1H - ^{13}C HMBC spectrum (500 MHz, CDCl_3) of crude poly(CS_2 -co-1). Reaction performed neat at 80 °C with $[\mathbf{1}]_0 : [\text{CS}_2]_0 : [\text{CrSalen}]_0 : [\text{PPNCl}]_0$ loadings of 100 : 200 : 1 : 1.

3.42–3.56 ppm, suggesting the occurrence of other polymer linkages (Fig. 2). While only resonances **S1** and **S2** were observed in the thiocarbonyl region of the $^{13}\text{C}\{^1\text{H}\}$ NMR spectrum of isolated poly(CS_2 -co-1) (Fig. 1e), a weak correlation between a xanthate-like ($\delta = 212.8$ ppm) and an e ($\delta = 3.42$ – 3.56 ppm) proton environment was detected by ^1H - ^{13}C $\{^1\text{H}\}$ NMR HMBC spectroscopy (Fig. 2c), revealing the presence of xanthate polymer linkages (e_{xanthate}). Conversely, no ^1H - ^{13}C $\{^1\text{H}\}$ NMR HMBC correlation was observed for the e proton environment detected at $\delta = 2.65$ – 3.13 ppm. Comparison with literature data³² revealed that the ^1H NMR and $^{13}\text{C}\{^1\text{H}\}$ NMR shift values of this resonance was comparable to known polythioethers (Fig. 2b),³⁶ corroborating the absence of a nearby

quaternary carbon. This resonance was therefore attributed to a thioether polymer linkage ($e_{\text{thioether}}$). The complexity of the signals seen may stem from random position of the thioether linkages in the polymer sequence. Regardless of the origins of those various linkages, the e environments in the ^1H NMR spectra were thus identified as an easy way to assess the selectivity of the ROCOP process.

Encouraged by this preliminary data, further catalytic ROCOP experiments were performed to study the effect of concentration, temperature, CS_2 stoichiometry and nature of the catalyst and of co-catalyst on the products of the ROCOP reaction (Table 1).

Impact of temperature on polymer linkages

Polymerisations were carried out at 25 °C, 60 °C, 80 °C, 100 °C and 140 °C at $[\mathbf{1}]_0 : [\text{CS}_2]_0 : [\text{CrSalen}]_0 : [\text{PPNCl}]_0$ loadings of 200 : 400 : 1 : 1 (Table 1, entries 1–5). **CrSalen** was found to be active for $\mathbf{1}/\text{CS}_2$ ROCOP at all temperatures tested, including at 25 °C (Table 1, entry 1). The room temperature reactivity of the $\text{CS}_2/\mathbf{1}$ ROCOP contrasts strongly with analogous reactions with cyclic anhydrides which necessitate high temperatures and long reaction times (100 °C, 2–6 days) to give similar oxetane conversions. Overall, the reactivity of **1** with CS_2 seems comparable with that of cyclohexene oxide,³⁰ cyclopentene oxide⁴² and oxetane,³² although direct comparisons of TOFs are not appropriate due to substantial differences in the reaction conditions used. The enhanced activity of **CrSalen** in the ROCOP of $\text{CS}_2/\mathbf{1}$ as compared with cyclic anhydrides may be a result of two effects. Firstly, CS_2 is a stronger electrophile than cyclic anhydrides owing to the lower enthalpy of the $\text{C}=\text{S}$ bond vs. the $\text{C}=\text{O}$ bond (573 and 799 kJ mol^{-1} , respectively).^{50,51} Secondly, following CS_2 insertion, the resulting thiocarbonate species are more nucleophilic than a carboxylate and the $\text{Cr}-\text{S}$ bond is likely less strong than a $\text{Cr}-\text{O}$ bond, which promotes propagation.

Within the limits of ^1H NMR spectroscopy, in all the experiments performed, all resonances seen could be assigned to poly(CS_2 -co-1) (as described above), cyclic xanthate **2** or oxetane monomer **1** (Fig. 1). However, varying the reaction temperature caused significant divergences in product distributions. Increasing the temperature resulted in a loss of regioselectivity (Table 1, entries 1–5 and Fig. S6†). At 25 °C, 60 °C and 80 °C, high HH/TT regioselectivity was observed (92, 85 and 89%, respectively, Table 1, entries 1–3). Conversely, for reactions performed at 100 °C and 140 °C, lower percentages of trithiocarbonates linkages were observed (73 and 57%, respectively, Table 1, entries 4 and 5) with an increase in thioether linkages detected (16% and 31%, respectively). The increased occurrence of thioether linkages at elevated temperatures likely arises from the elimination of COS from propagation intermediates, favoured by entropy (Scheme S2†) and as noted in previous studies.^{30,32,42} The ratio of xanthate links also increased with temperature, but to a lesser extent than for the thioethers (6% at 25 °C up to 12% at 140 °C, Table 1 entries 1–5). The formation of xanthate linkages may be a result of several mechanisms: the ‘expected’ $\text{CS}_2/\mathbf{1}$ ROCOP, but



Table 1 Optimization of the ROCOP of 1 with CS₂

Entry	T (°C)	[1] ₀ : [CS ₂] ₀ : [cat] ₀ : [co-cat] ₀	Cat.	Co-catalyst	% conv. of 1 ^a	% 2 ^b	% poly (CS ₂ -co-1) ^b	Polymer linkages ratio n : m : l ^c	M _{n,SEC} [D _M] (g mol ⁻¹) ^d
1 ^e	25	200 : 400 : 1 : 1	CrSalen	PPNCI	61	4	96	92 : 6 : 2	8700 [1.70]
2 ^f	60	200 : 400 : 1 : 1	CrSalen	PPNCI	88	15 {10}	85 {90}	85 : 9 : 6 {59 : 10 : 31}	12 000 [1.77] {5300 [2.02]}
3	80	200 : 400 : 1 : 1	CrSalen	PPNCI	100	13	77	89 : 9 : 2	15 000 [2.13]
4	100	200 : 400 : 1 : 1	CrSalen	PPNCI	100	14	76	73 : 11 : 16	7700 [1.63]
5	140	200 : 400 : 1 : 1	CrSalen	PPNCI	100	38	62	57 : 12 : 31	6300 [1.93]
6	80	200 : 100 : 1 : 1	CrSalen	PPNCI	58	34	66	56 : 7 : 36	2700 [1.68]
7	80	200 : 200 : 1 : 1	CrSalen	PPNCI	100	22	78	82 : 10 : 8	9100 [1.76]
8	80	200 : 800 : 1 : 1	CrSalen	PPNCI	100	10	90	95 : 5 : 0	14 000 [1.78]
9	80	200 : 400 : 1 : 1	CoSalen	PPNCI	0	—	—	—	—
10	80	200 : 400 : 1 : 1	AlSalen	PPNCI	1	—	—	—	—
11	25	200 : 400 : 1 : 1	AlTris	PPNCI	12	8	92	—	—
12	80	200 : 400 : 1 : 1	AlTris	PPNCI	100	19	81	75 : 10 : 15	6300 [1.69]
13	100	200 : 400 : 1 : 1	AlTris	PPNCI	100	52	48	55 : 7 : 38	2200 [1.53]
14	80	200 : 400 : 1 : 5	LZn ₂ Ph ₂	CHD	1	—	—	—	—
15	80	200 : 400 : 1 : 1	KOtBu	18-Crown-6	2	—	—	—	—
16	80	200 : 400 : 1 : 0	CrSalen	—	8	43	57	—	—
17	80	200 : 400 : 0 : 1	—	PPNCI	0	—	—	—	—
18	80	200 : 400 : 1 : 1	CrSalen	NBu ₄ Cl	91	16	84	91 : 5 : 4	6600 [2.00]
19	80	200 : 400 : 1 : 1	CrSalen	NBu ₄ Br	4	—	—	—	—
20	80	200 : 400 : 1 : 1	CrSalen	NBu ₄ I	51	31	69	77 : 11 : 12	4700 [1.77]
21	110	200 : 400 : 1 : 1	CrSalen	PPNCI	100	35	65	66 : 11 : 23	4400 [1.58]
22 ^g	110	200 : 400 : 1 : 1	CrSalen	PPNCI	100	58	42	47 : 8 : 45	1700 [1.33]
23 ^h	110	200 : 400 : 1 : 1	CrSalen	PPNCI	93	65	35	39 : 10 : 51	1400 [1.28]
24 ⁱ	110	200 : 400 : 1 : 1	CrSalen	PPNCI	33	52	48	—	—

Reactions carried out in σ -dichlorobenzene at [1]₀ = 1.34 mol L⁻¹ over 20 h unless stated otherwise. ^a Conversion of 1 determined by ¹H NMR spectroscopy in CDCl₃ using relative integration of anomeric protons in 1 (δ = 6.26 ppm (d, J = 3.7 Hz, 1H)), poly(CS₂-co-1) (δ = 5.88–5.99 ppm (1H)), and 2 (CDCl₃, δ = 6.03 ppm (d, J = 3.7 Hz, 1H)). ^b Calculated by ¹H NMR spectroscopy using relative integration of anomeric protons in poly(CS₂-co-1) and 2. ^c Calculated by ¹H NMR spectroscopy in CDCl₃ using relative integration of e environments (CH₂) assigned to HH/TT trithiocarbonate linkages n (δ = 3.68 ppm (h, J = 6.9 Hz, 4H)), HT xanthate linkages m (δ = 3.51 ppm (t, J = 6.6 Hz, 2H)) and thioether linkages l (δ = 3.04–2.74 ppm (m, 2H)). ^d Calculated by SEC relative to polystyrene standards in THF eluent; $D_M = M_w/M_n$. ^e Time = 309 h. ^f Bracketed values taken at 119 h. ^g [1]₀ = 0.67 mol L⁻¹. ^h [1]₀ = 0.335 mol L⁻¹. ⁱ 0.08 mol L⁻¹.

also various S/O rearrangements occurring during ROCOP,²⁷ including transthiocarbonation between polymer chains, as well as the regioregular ROP of 2 (Schemes S1 and S2†).

At 80 °C, quantitative conversion of 1 was observed after 20 h, yielding the maximum molar mass of polymer achieved under the conditions tested (15 000 g mol⁻¹, D_M = 2.13, Table 1, entry 3). More generally, obtained $M_{n,SEC}$ values were far from $M_{n,theo}$, likely due to residual protic impurities (e.g. 1,2-O-isopropylidene-D-xylofuranose) in the monomer samples

which may act as chain transfer agents to decrease the molar mass of the polymers. This is typical within the field of cyclic ether/CS₂ ROCOP.^{30,32,42} Further purification of 1, including *via* successive or reactive distillation with NaH/MeI,⁵² unfortunately did not increase the polymer molar masses. While analysis of the polymer by MALDI ToF mass spectrometry proved unsuccessful, end-group titration by ³¹P NMR spectroscopy indicated that some of the polymer chains were linear and terminated by secondary alcohol end groups (Fig. S24 and S2†).



Increasing the temperature to 100 °C and 140 °C, also resulted in quantitative conversion of **1**, although the polymer molar masses were lower (7700 g mol⁻¹, $D_M = 1.63$ and 6300, $D_M = 1.93$, Table 1 entries 4 and 5, respectively). At these temperatures, several factors may be responsible for a decrease in molar mass, including the increased occurrence of thioether linkages (concurrent with loss of COS) in the polymer, and the decreased reaction selectivity towards polymer (in favour of cyclic monomer **2**), in line with thermodynamics principles.

The reaction at 60 °C was monitored for up to 5 days to assess the impact of longer reaction times on the polymer linkages and molar mass (Table 1, entry 2). A decrease in molar mass and increasing thioether linkages were observed, suggesting decarbonylsulfonation of the polymer chains upon extended heating.

Impact of CS₂ stoichiometry and co-catalyst

The impact of CS₂ loadings on product distributions and ROCOP regioselectivity was next investigated (Table 1, entries 1 and 6–8). The reactions were performed at 80 °C with a [1]₀: [CrSalen]₀: [PPNCl] feed ratio of 200:1:1. At [1]₀: [CS₂]₀ ratio of 2:1, conversion of **1** was limited to 58% after 20 h (Table 1, entry 6). Selectivity for alternating linkages also decreased significantly with a concurrent increase in thioether links (56% and 36%, respectively), as compared with the analogous reaction performed with a [1]₀: [CS₂]₀ ratio of 1:2. Given that the homopolymerisation of **1** is kinetically inaccessible at 80 °C with a CrSalen/PPNCl catalyst, this clearly suggests some S–O exchange reactions, which either progressively liberate COS/CS₂ so that ROCOP can continue beyond 50% conversion, or which form a thietane prone to ROP under these conditions. Reactions performed with [1]₀: [CS₂]₀ ratio of 1:1 and 1:4 gave quantitative conversion of **1** and an increased percentage of alternating links (87% and 95%, respectively, Table 1, entries 7 and 8). Similar observations have been made previously in the oxetane/CS₂ ROCOP, with higher loadings of CS₂ shown to inhibit S/O exchange reactions.³² Moreover, the amount of **2** decreased with increasing [CS₂]₀ (Table 1, entries 6–8): high concentrations of CS₂ would likely favour insertion into propagating chains over backbiting reactions.

Impact of the nature of ROCOP catalyst and co-catalyst

The use of AlSalen (Al(III)) and CoSalen (Co(II)) complexes failed to give any conversion of **1** under the screened conditions (Table 1, entries 9 and 10). Conversely, the trisphenolate complex, AlTris (Al(III)), was found to be active at 25 °C, 80 °C and 100 °C, although, as compared with the analogous CrSalen reactions, the product microstructure was less regioregular and the molar masses of the polymer were lower (Table 1, entries 11–13). Dizinc complex, LZn₂Ph₂ (with 1,2-cyclohexandiol (CHD) chain transfer agent) and alkoxide/crown-ether initiator gave no conversion of **1** (Table 1, entries 14 and 15). Lastly, no conversion of **1** was noted in when using only the PPNCl co-catalyst, whilst when performing the reaction with just CrSalen, poor conversion of **1** was obtained as

compared with the standard conditions (Table 1, entries 16 and 17).

The effect of the co-catalyst nature was next studied (Table 1, entries 18–20). A reaction performed with NBu₄Cl at 80 °C with [1]₀: [CS₂]: [CrSalen]₀: [NBu₄Cl]₀ loadings of 200:400:1:1 gave 91% conversion of **1** with comparable selectivity ratios to those observed with PPNCl (Table 1, entry 18), albeit with lower molar mass polymer obtained (6600 vs. 15 000 g mol⁻¹ in entry 3). Conversely, a copolymerisation carried out with NBu₄Br gave only 4% conversion, indicating the bromide salt is unsuitable for 1/CS₂ ROCOP (Table 1, entry 19). Under similar conditions, NBu₄I gave improved conversion of **1** although with lower activity than observed with PPNCl and NBu₄Cl (Table 1, entry 20). An increased amount of **2** was also observed suggesting that iodide may promote backbiting.

Collectively, these data thus identified CrSalen/PPNCl as the optimal binary catalytic system for 1/CS₂ ROCOP so far, in terms of activity, polymer molar mass, and regioselectivity of the polymer linkages.

Optimisation of reaction conditions towards formation of **2**

Although the reaction selectivity could not be tailored towards exclusive formation of **2**, 1/CS₂ cycloaddition could be promoted over ROCOP at high temperatures and low [1]₀. At 110 °C and [1]₀ = 0.335 mol L⁻¹, formation of up to 65% of **2** was observed (Table 1 entries 21–23). Monomer grade xanthate **2** could then be easily isolated using a simple filtration of the reaction mixture on silica, leading to isolated yields of up to 60%, a considerable improvement on the previous report (15% yield).²⁷ Unfortunately, a further decrease in [1]₀ to 0.08 mol L⁻¹ led to a significant drop in catalyst activity and poor conversions of **1** (33%; Table 1, entry 24).

Kinetic and mechanistic studies

Considering the presence of **2** in all ROCOP reactions performed, it can be envisaged that the formation of poly(CS₂-co-**1**) does not proceed directly but stepwise, first by the cycloaddition of CS₂ and **1** into **2**, then ROP of **2** (Fig. 3). This would be analogous to what has been reported in the coupling of CO₂ and oxetanes by Darensbourg,^{53–56} and by Dove and Coulembier.⁵⁷ A reaction performed at [2]₀: [CrSalen]₀: [PPNCl]₀ loadings of



Fig. 3 Possible pathways for the formation of poly(CS₂-co-**1**) and **2**.



Table 2 ROP of **2** and depolymerisation of poly(**CS**₂-co-**1**)

Entry	T (°C)	Reagent	% ^a Conv	% ^b Polym	<i>n</i> : <i>m</i> : <i>l</i> ^c	<i>M</i> _{n,SEC} [<i>D</i> _M] ^d
1 ^e (ref. 27)	25	2	86	86	87 : 10 : 3	10 600 [1.5]
2	80	2	75	75	85 : 12 : 3	12 700 [2.05]
3 ^f	80	Poly(CS ₂ -co- 1)	0	100	76 : 8 : 16	8200 [1.70]
4 ^f	110	Poly(CS ₂ -co- 1)	45	55	65 : 10 : 25	3600 [1.62]
5 ^f	140	Poly(CS ₂ -co- 1)	— ^g	—	—	—

Reactions carried out for 20 h in σ -dichlorobenzene with $[2/1_{\text{monomer unit}}]_0 : [\text{CrSalen}]_0 : [\text{PPNCl}]_0$ loadings of 200 : 1 : 1, and $[2/1_{\text{monomer unit}}]_0 = 1.34 \text{ mol L}^{-1}$ unless otherwise stated. ^a Conversion of substrate determined by ¹H NMR spectroscopy in CDCl₃ using relative integration of anomeric protons (1H) in substrates and products (**1**: $\delta = 6.26 \text{ ppm}$ (d, $J = 3.7 \text{ Hz}$)); poly(**CS**₂-co-**1**): $\delta = 5.88\text{--}5.99 \text{ ppm}$; **2**: $\delta = 6.03 \text{ ppm}$ (d, $J = 3.7 \text{ Hz}$). ^b Calculated by ¹H NMR spectroscopy using relative integration of anomeric protons in poly(**CS**₂-co-**1**) and **2**. ^c Calculated by ¹H NMR spectroscopy in CDCl₃ using relative integration of *e* environments (CH₂) assigned to HH/TT trithiocarbonate linkages *n* ($\delta = 3.68 \text{ ppm}$ (h, $J = 6.9 \text{ Hz}$, 4H)), HT xanthate linkages *m* ($\delta = 3.51 \text{ ppm}$ (t, $J = 6.6 \text{ Hz}$, 2H)) and thioether linkages *l* ($\delta = 3.04\text{--}2.74 \text{ ppm}$ (m, 2H)). ^d Calculated by SEC relative to polystyrene standards in THF eluent; $D_M = M_w/M_n$. ^e Reaction performed with $[2]_0 : [\text{TBD}]_0 : [4\text{-MeBnOH}]_0$ loadings of 100 : 1 : 1 in DCM with $[2]_0 = 1.0 \text{ mol L}^{-1}$, time = 15 minutes. ^f Substrate polymer data: *n* : *m* : *l* ratio = 82 : 6 : 12; $M_{n,SEC} = 8500 \text{ g mol}^{-1}$. ^g Insoluble black residue formed during 20 h reaction.

200 : 1 : 1 gave 75% conversion of **2** into a polymer with similar microstructure, molar mass and D_M values to those obtained previously *via* reaction of **1** with CS₂ (Table 2, entry 1 vs. Table 1, entry 3). In addition, the final product distribution matched well that observed in 1/CS₂ ROCOP (around 75 : 25 polymer : cyclic monomer ratio). This demonstrates that ROP of xanthate **2** is accessible at 80 °C with the CrSalen/PPNCl catalyst system.

In order to probe whether the copolymerisation of CS₂/1 occurred *via* ROP of **2**, reaction monitoring by ¹H NMR spec-

troscopy was performed at 25 °C, 80 °C and 110 °C with $[1]_0 : [\text{CS}_2]_0 : [\text{CrSalen}]_0 : [\text{PPNCl}]_0$ loadings of 200 : 400 : 1 : 1 (Fig. 4). At 80 °C, inspection of the early stages (<1 h) of the reaction revealed that polymer and **2** formed at approximately the same rate (Fig. 4a). After 1–2 h, the concentration of **2** plateaued as the polymer concentration increased.

At 110 °C, simultaneous rapid formation of both the polymer and cyclic xanthate was also observed (Fig. 4c), whereas at 25 °C, minimal xanthate was detected across several days (Fig. 4d). An experiment to monitor the ROP of **2**



Fig. 4 Time vs. conversion of **1** (black, square) and formation of xanthate **2** (red, circle) and poly(**CS**₂-co-**1**) (blue, triangle) determined by ¹H NMR spectroscopy for reactions performed in σ -dichlorobenzene with $[1]_0 : [\text{CS}_2]_0 : [\text{CrSalen}]_0 : [\text{PPNCl}]_0$ loadings of 200 : 400 : 1 : 1 with $[1]_0 = 1.34 \text{ mol L}^{-1}$ at (a) 80 °C; (c) 110 °C and (d) 25 °C. (b) Relative rates of poly(**CS**₂-co-**1**) formation (determined by ¹H NMR spectroscopy) at 80 °C in the ROCOP of **1** and CS₂ (red, circle, $[1]_0 : [\text{CS}_2]_0 : [\text{CrSalen}]_0 : [\text{PPNCl}]_0$ loadings of 200 : 400 : 1 : 1 with $[1]_0 = 1.34 \text{ mol L}^{-1}$) and in the ROP of **2** (black, square, with $[2]_0 : [\text{CS}_2]_0 : [\text{CrSalen}]_0 : [\text{PPNCl}]_0$ loadings of 200 : 200 : 1 : 1 with $[2]_0 = 1.34 \text{ mol L}^{-1}$).



was also performed at 80 °C, with [2]₀: [CS₂]₀: [CrSalen]₀: [PPNCl]₀ loadings of 200:200:1:1 in the presence of a alcohol initiator, 4-MeBnOH. CS₂ and 4-MeBnOH were added to the reaction mixture in attempt to simulate ROCOP conditions, in which excess CS₂ and polymer growing chains are present in solution. Assuming first order kinetics in monomer, the rate of polymer formation was slower in the ROP of **2** than in the 1/CS₂ ROCOP (Fig. 4b). With no build-up of **2** seen during ROCOP, this data therefore suggest that polymer is formed at least partially *via* direct ROCOP.

2 could also be formed *via* back-biting of the polymer chains (Fig. 3). A reaction performed at 80 °C with isolated polymer as substrate, at [poly(CS₂-co-1)]₀: [CrSalen]₀: [PPNCl]₀ loadings of 200:1:1, gave no formation of cyclic xanthate after 20 h (Table 2, entry 3). This suggests that at 80 °C, cycloaddition of **1** and CS₂ is the dominant mechanism for formation **2**. However, at 110 °C, back-biting was observed, with approximately 45% xanthate formed after 20 h. No other cyclic species were detected in solution (Table 2, entry 4). The polymer molar mass also decreased from 8500 g mol⁻¹ to 3600 g mol⁻¹, corroborating the loss of **2** from polymer chains. Increasing the temperature further to 140 °C led to formation of a black, insoluble residue (Table 2, entry 5). SEC analysis of the THF-soluble fraction indicated the presence of oligomers only. These data suggest that at elevated temperatures, alternative depolymerisation mechanisms are operative leading to significant, uncontrolled, polymer degradation.

Thermal properties of the polymers

Thermal analysis of the polymers with a range of *n*:*m*:*l* ratios was undertaken to understand the impact of varying polymer linkage on properties (Table 3, Fig. S7–15†). All polymers analysed were found to have temperatures of onset of degradation (*T*_{d,onset}) of between 167–208 °C. Glass transition temperatures (*T*_g) were between 108–137 °C, higher than those reported previously,²⁷ but mostly lower than those reported for the analogous, fully oxygenated polycarbonate developed by Gross and

co-workers (*T*_g = 128 °C).⁵⁸ Contrasting with earlier studies which showed a clear impact of sulfur content on polymer properties,^{30,42} no general trend between the polymer microstructure and thermal properties was observed. However, as samples of similar molar masses could not be obtained and compared, any existing relationship may be overshadowed by the effect of chain length variations. No crystallinity was detected by differential scanning calorimetry (DSC) or wide-angle X-ray scattering (WAXS) analysis (Fig. S16†).

Degradability of the polymers

A potential advantage of sulfur-containing analogues of polycarbonates is that their degradation into small molecules may be possible under UV light. For example, a catalyst-free method for removal of trithiocarbonate RAFT chain transfer agents from poly(vinylpyridine)s has recently been developed



Fig. 5 SEC traces following exposure of poly(CS₂-co-1) (*M*_{n,SEC} = 8400, *D*_M = 1.67) to UV (*λ* = 365 nm) in the presence of (a) TTMSS (7.5 monomer equiv.) and (b) with no silane present. The reactions were performed at room temperature with [poly(CS₂-co-1)]₀ = 0.0267 mol L⁻¹.

Table 3 Impact of poly(CS₂-co-1) linkage ratio (*n*:*m*:*l*) on polymer thermal properties

Entry	<i>n</i> : <i>m</i> : <i>l</i> ^a	<i>M</i> _{n,SEC} [<i>D</i> _M] (g mol ⁻¹) ^b	<i>T</i> _{d,onset} (°C)	<i>T</i> _{d5} (°C)	<i>T</i> _g (°C)
1	95:5:0	14 000 [1.78]	188	216	114
2	89:9:2	15 400 [2.13]	167	190	110
3	87:10:3	9100 [1.78]	191	216	108
4	69:17:14	14 400 [1.27]	208	257	137
5	61:5:34	14 000 [1.19]	172	186	117
6	57:12:31	8400 [1.67]	178	209	120

^a Calculated by ¹H NMR spectroscopy in CDCl₃ using relative integration of *e* environments (CH₂) assigned to HH/TT trithiocarbonate linkages *n* (*δ* = 3.68 ppm (h, *J* = 6.9 Hz, 4H)), HT xanthate linkages *m* (*δ* = 3.51 ppm (t, *J* = 6.6 Hz, 2H)) and thioether linkages *l* (*δ* = 3.04–2.74 ppm (m, 2H)). ^b Calculated by SEC relative to polystyrene standards in THF eluent; *D*_M = *M*_w/*M*_n.



by Kennemur and co-workers.²¹ It was envisioned that such method may also affect the trithiocarbonate linkages in poly(CS₂-co-1). A reaction performed in THF with 7.5 monomer equivalents of tris(trimethylsilyl)silane (TTMSS) led to oligomeric products after approximately 10 min of UV irradiation ($\lambda = 365$ nm; Fig. 5a). Further analysis of the degradation products by ¹H NMR spectroscopy proved challenging (Fig. S20†). A control experiment performed in the absence of TTMSS resulted in degradation of poly(CS₂-co-1) too, albeit at a slower rate, as inferred from SEC traces (Fig. 5b). Under these conditions, up to 12% formation of xanthate 2 was also observed by ¹H NMR spectroscopy after 1 hour, before degrading progressively along with poly(CS₂-co-1).

Conclusions

The ROCOP of CS₂ with an anhydro-functionalised xylofuranose derivative has been reported. Through variation of the reaction parameters (*e.g.* temperature and CS₂ stoichiometry), some control over the regioselectivity and the nature of the polymer linkages is possible. Conditions can also be tailored to enable the isolation of a polymerisable cyclic xanthate with good yields. Chemical recycling and degradation of the polymers have also been demonstrated. Further investigations are ongoing to develop a deeper understanding of the polymerisation mechanism, of the sulfur/oxygen exchange reactions, and of the impact of the polymer sequence on physical properties.

Conflicts of interest

There are no conflicts to declare.

Acknowledgements

Analytical facilities were provided through the Material and Chemical Characterisation Facility at the University of Bath. We thank the UK EPSRC (EP/N022793/1, DTP studentship for T.M.G.), as well as the Royal Society (UF/160021 fellowship to A.B.) for research funding.

Notes and references

- G. L. Gregory, E. M. López-Vidal and A. Buchard, *Chem. Commun.*, 2017, **53**, 2198–2217.
- J. J. Bozell and G. R. Petersen, *Green Chem.*, 2010, **12**, 539–554.
- F. Fenouillot, A. Rousseau, G. Colomines, R. Saint-Loup and J. P. Pascault, *Prog. Polym. Sci.*, 2010, **35**, 578–622.
- J. A. Galbis, M. d. G. García-Martín, M. V. de Paz and E. Galbis, *Chem. Rev.*, 2016, **116**, 1600–1636.
- R. Xiao and M. W. Grinstaff, *Prog. Polym. Sci.*, 2017, **74**, 78–116.
- S. E. Felder, M. J. Redding, A. Noel, S. M. Grayson and K. L. Wooley, *Macromolecules*, 2018, **51**, 1787–1797.
- A. T. Lonnecker, Y. H. Lim and K. L. Wooley, *ACS Macro Lett.*, 2017, **6**, 748–753.
- K. Mikami, A. T. Lonnecker, T. P. Gustafson, N. F. Zinnel, P.-J. Pai, D. H. Russell and K. L. Wooley, *J. Am. Chem. Soc.*, 2013, **135**, 6826–6829.
- Y. Shen, X. Chen and R. A. Gross, *Macromolecules*, 1999, **32**, 2799–2802.
- J. Kawada, T. Lütke-Eversloh, A. Steinbüchel and R. H. Marchessault, *Biomacromolecules*, 2003, **4**, 1698–1702.
- M. Luo, X.-H. Zhang and D. J. Darensbourg, *Acc. Chem. Res.*, 2016, **49**, 2209–2219.
- B. Ochialy and T. Endo, *Prog. Polym. Sci.*, 2005, **30**, 183–215.
- H.-L. Wu, J.-L. Yang, M. Luo, R.-Y. Wang, J.-T. Xu, B.-Y. Du, X.-H. Zhang and D. J. Darensbourg, *Macromolecules*, 2016, **49**, 8863–8868.
- M. Kato, K. Toshima and S. Matsumura, *Biomacromolecules*, 2007, **8**, 3590–3596.
- J.-L. Yang, Y. Wang, X.-H. Cao, C.-J. Zhang, Z. Chen and X.-H. Zhang, *Macromol. Rapid Commun.*, 2021, **42**, 2000472.
- H. R. Kricheldorf and G. Schwarz, *J. Macromol. Sci., Part A: Pure Appl. Chem.*, 2007, **44**, 625–649.
- E. Marianucci, C. Berti, F. Pilati, P. Manaresi, M. Guaita and O. Chiantore, *Polymer*, 1994, **35**, 1564–1566.
- R. K. Sadhir and K. F. Schoch, *Chem. Mater.*, 1996, **8**, 1281–1286.
- A. Kultys, in *Encyclopedia of Polymer Science and Technology*, 2010, DOI: 10.1002/0471440264.pst355.pub2.
- S. Wu, M. Luo, D. J. Darensbourg and X. Zuo, *Macromolecules*, 2019, **52**, 8596–8603.
- B. A. Fultz, D. Beery, B. M. Coia, K. Hanson and J. G. Kennemur, *Polym. Chem.*, 2020, **11**, 5962–5968.
- L. Tagle, F. Diaz and P. Riveros, *Polym. J.*, 1986, **18**, 501–504.
- L. Tagle, F. Diaz and P. Salas, *J. Macromol. Sci., Part A: Pure Appl. Chem.*, 1989, **26**, 1321–1334.
- L. H. Tagle, F. R. Diaz, J. C. Vega and P. F. Alquinta, *Makromol. Chem.*, 1985, **186**, 915–921.
- C. Berti, E. Marianucci and F. Pilati, *Makromol. Chem.*, 1988, **189**, 1323–1330.
- W. Choi, F. Sanda and T. Endo, *Macromolecules*, 1998, **31**, 9093–9095.
- E. M. López-Vidal, G. L. Gregory, G. Kociok-Köhn and A. Buchard, *Polym. Chem.*, 2018, **9**, 1577–1582.
- Y.-Z. You, C.-Y. Hong and C.-Y. Pan, *Macromol. Rapid Commun.*, 2002, **23**, 776–780.
- A. W. M. Lee, W. H. Chan and H. C. Wong, *Synth. Commun.*, 1988, **18**, 1531–1536.
- D. J. Darensbourg, J. R. Andreatta, M. J. Jungman and J. H. Reibenspies, *Dalton Trans.*, 2009, 8891–8899.
- J. Diebler, H. Komber, L. Häußler, A. Lederer and T. Werner, *Macromolecules*, 2016, **49**, 4723–4731.
- M. Luo, X.-H. Zhang and D. J. Darensbourg, *Macromolecules*, 2015, **48**, 5526–5532.



- 33 J.-L. Yang, L.-F. Hu, X.-H. Cao, Y. Wang and X.-H. Zhang, *Chin. J. Chem.*, 2020, **38**, 269–274.
- 34 Y. Li, H.-Y. Duan, M. Luo, Y.-Y. Zhang, X.-H. Zhang and D. J. Darensbourg, *Macromolecules*, 2017, **50**, 8426–8437.
- 35 T.-J. Yue, W.-M. Ren, Y. Liu, Z.-Q. Wan and X.-B. Lu, *Macromolecules*, 2016, **49**, 2971–2976.
- 36 C.-J. Zhang, T.-C. Zhu, X.-H. Cao, X. Hong and X.-H. Zhang, *J. Am. Chem. Soc.*, 2019, **141**, 5490–5496.
- 37 T.-J. Yue, W.-M. Ren, L. Chen, G.-G. Gu, Y. Liu and X.-B. Lu, *Angew. Chem., Int. Ed.*, 2018, **57**, 12670–12674.
- 38 J.-L. Yang, H.-L. Wu, Y. Li, X.-H. Zhang and D. J. Darensbourg, *Angew. Chem., Int. Ed.*, 2017, **56**, 5774–5779.
- 39 S. Paul, Y. Zhu, C. Romain, R. Brooks, P. K. Saini and C. K. Williams, *Chem. Commun.*, 2015, **51**, 6459–6479.
- 40 A. Plajer and C. K. Williams, *Angew. Chem., Int. Ed.*, 2021, DOI: 10.1002/anie.202104495.
- 41 X.-H. Zhang, F. Liu, X.-K. Sun, S. Chen, B.-Y. Du, G.-R. Qi and K. M. Wan, *Macromolecules*, 2008, **41**, 1587–1590.
- 42 D. J. Darensbourg, S. J. Wilson and A. D. Yeung, *Macromolecules*, 2013, **46**, 8102–8110.
- 43 M. J. H. Worthington, R. L. Kucera and J. M. Chalker, *Green Chem.*, 2017, **19**, 2748–2761.
- 44 J. M. Chalker, M. J. H. Worthington, N. A. Lundquist and L. J. Esdaile, *Top. Curr. Chem.*, 2019, **377**, 16.
- 45 X. Wu, J. A. Smith, S. Petcher, B. Zhang, D. J. Parker, J. M. Griffin and T. Hasell, *Nat. Commun.*, 2019, **10**, 647.
- 46 T. M. McGuire, J. Bowles, E. Deane, E. H. E. Farrar, M. N. Grayson and A. Buchard, *Angew. Chem., Int. Ed.*, 2021, **60**, 4524–4528.
- 47 T. M. McGuire, E. F. Clark and A. Buchard, *Macromolecules*, 2021, **54**, 5094–5105.
- 48 T. Uryu, Y. Koyama and K. Matsuzaki, *Makromol. Chem.*, 1984, **185**, 2099–2107.
- 49 T. Uryu, Y. Koyama and K. Matsuzaki, *J. Polym. Sci., Polym. Lett. Ed.*, 1979, **17**, 673–678.
- 50 D. Stevenson, *J. Am. Chem. Soc.*, 1955, **77**, 2350–2350.
- 51 B. d. Darwent, in *National Bureau of Standards*, 1970, vol. 31, pp. 15–22.
- 52 O. Hauenstein, M. Reiter, S. Agarwal, B. Rieger and A. Greiner, *Green Chem.*, 2016, **18**, 760–770.
- 53 D. J. Darensbourg and A. I. Moncada, *Macromolecules*, 2010, **43**, 5996–6003.
- 54 D. J. Darensbourg, A. I. Moncada and S.-H. Wei, *Macromolecules*, 2011, **44**, 2568–2576.
- 55 G. A. Bhat, M. Luo and D. J. Darensbourg, *Green Chem.*, 2020, **22**, 7707–7724.
- 56 D. J. Darensbourg, A. I. Moncada, W. Choi and J. H. Reibenspies, *J. Am. Chem. Soc.*, 2008, **130**, 6523–6533.
- 57 J. Huang, J. De Winter, A. P. Dove and O. Coulembier, *Green Chem.*, 2019, **21**, 472–477.
- 58 Y. Shen, X. Chen and R. A. Gross, *Macromolecules*, 1999, **32**, 2799–2802.

